

High-sensitivity detection of CH radicals in flames by use of a diode-laser-based near-ultraviolet light source

Kristen A. Peterson and Daniel B. Oh

Southwest Sciences, Inc., 1570 Pacheco Street, Suite E-11, Santa Fe, New Mexico 87505

Received January 28, 1999

CH radical distributions in ethylene-air and methane-air diffusion flames are mapped by wavelength-modulation absorption spectroscopy (WMS). Tunable, wavelength-modulated 426-nm light is generated by frequency doubling of a modulated 852-nm distributed Bragg reflector diode laser. Absorbances of 5×10^{-5} are measured with second-harmonic ($2f$) WMS with a signal-to-noise ratio of 3:1 in a 3-Hz measurement bandwidth. The feasibility of simultaneous line-of-sight absorption and spatially resolved laser-induced fluorescence detection with a single excitation beam is also demonstrated. This near-UV source is suitable for microgravity drop-tower experiments and other applications in which compact, rugged, energy-efficient instrumentation is required. © 1999 Optical Society of America

OCIS codes: 120.1740, 190.2620, 140.2020, 300.6380, 120.1880.

Quantitative mapping of combustion species with good spatial resolution is essential for improved understanding of flame chemical kinetics and fluid dynamics. Laser-induced-fluorescence (LIF) spectroscopy has been a main staple of combustion diagnostics because of its high detection sensitivity, selectivity, and excellent spatial resolution. However, extracting quantitative species densities from LIF measurements requires careful calibration of geometric factors and laser intensity, as well as modeling of fluorescence quenching by collision partners. This has been challenging even under the most favorable conditions.¹

Wavelength-modulation absorption spectroscopy (WMS) provides quantitative, high-sensitivity detection of trace species² and is used in a diverse range of applications, including combustion studies.^{3,4} Minimum detectable absorbances of 10^{-6} have been demonstrated with current-modulated diode lasers.²⁻⁴ This method provides integrated absorbance along a line-of-sight optical path. However, it would be desirable to characterize the distribution along this line of sight.

LIF detection perpendicular to the laser beam can be used to map relative species densities along the line of sight, and the integrated absorption that is available through WMS provides a mathematical constraint on the extraction of quantitative information from the LIF data. Combining absorption with LIF—especially if the measurements are made simultaneously with the same excitation beam—may eliminate geometric factors and the effects of intensity fluctuations from the analysis.

To demonstrate the feasibility of simultaneous WMS and LIF detection of flame species, we have developed a tunable, wavelength-modulated near-UV source based on single-pass frequency doubling of a modulated near-IR diode laser. Most near-IR diode-laser-based blue or near-UV generation schemes use resonant cavity designs to increase the circulating pump power, resulting in high conversion efficiency but with the penalty of fixed output wavelength.⁵ Although the conversion efficiency is smaller in single-pass transmission of the pump beam, the resultant near-UV beam is readily tunable and wavelength modulated by variation and

modulation of the pump diode-laser current. Simultaneous WMS and LIF measurement with this light source is demonstrated by detection of CH radicals in diffusion flames.

The CH radical is chosen because of its importance in hydrocarbon flame chemistry, its role in soot formation, and its use as a marker of flame fronts.⁶ Rotationally resolved transitions of the $A^2\Delta \leftarrow X^2\Pi$ band near 430 nm and the $B^2\Sigma^- \leftarrow X^2\Pi$ band near 385 nm have been assigned⁷ and are utilized by many workers using LIF techniques.^{6,8-10} For detection in the $A^2\Delta \leftarrow X^2\Pi$ band, light near 426 nm is generated by means of doubling a high-power 852-nm distributed Bragg reflector diode laser (SDL 5722) in a nonlinear crystal.

Figure 1 shows a schematic of the experimental arrangement. The diode-laser beam (120 mW) is collimated, circularized with an anamorphic prism pair, and focused into a 7-mm-long A-cut KNbO₃ crystal. An optical isolator between the diode laser and the doubling crystal minimizes feedback from optical backreflections, and a half-wave plate before the crystal matches the input polarization of the

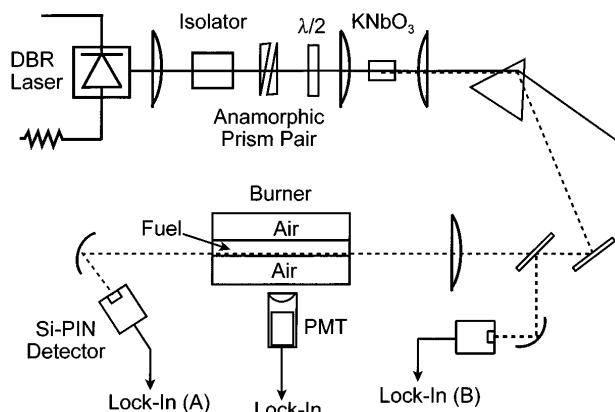


Fig. 1. Experimental schematic for 426-nm beam generation and CH detection by WMS absorption and LIF in a slot burner. DBR, distributed Bragg reflector; PMT, photomultiplier tube.

pump beam to the crystal orientation. The KNbO_3 crystal is mounted upon a thermoelectric cooling stage in an N_2 -purged housing for temperature-tuned noncritical phase-matching operation near 10°C . The 426-nm beam is collimated and separated from the residual 852-nm pump beam with a CaF_2 prism. The frequency of the residual pump beam is monitored to within 0.01 cm^{-1} with a scanning interferometer (Burleigh Wavemeter). The near-IR power input to the crystal is 85 mW, from which $100\ \mu\text{W}$ at 426 nm is produced. The UV power is very stable, without optics adjustments, as long as the crystal temperature is stabilized to within $\pm 0.1^\circ\text{C}$.

The output wavelength of the distributed Bragg reflector laser diode is tuned by adjustment of its temperature and injection current. The $R_2(8)$ (23460.81-cm^{-1}) line in the (0, 0) band of the CH $A^2\Delta \leftarrow X^2\Pi$ transition⁷ was chosen for the present study. In addition to several CH lines in this (0, 0) band, the frequency-doubled laser can provide access to some lines in the (1, 1) band that would allow optical thermometry¹¹ in a future study. The diode-laser injection current is modulated at 50 kHz, resulting in wavelength modulation of the frequency-doubled beam. A linear current sweep is also applied to the diode laser, providing a means to tune the center frequency across the absorption line during wavelength modulation.

The 426-nm beam is directed along the flame front of a Wolfard–Parker slot burner⁶ and is focused to $\sim 250\text{-}\mu\text{m}$ diameter at the center and $\sim 330\text{-}\mu\text{m}$ diameter on either side of the 4-cm-long burner. The transmitted beam intensity is monitored with a UV-grade Si p-i-n photodiode and sent to a digital lock-in amplifier (SRS 830) for $2f$ detection at 100 kHz. A Schott BG-18 blue pass filter is used to reduce the amount of visible and near-IR flame luminescence reaching the detector. Phase-sensitive detection of LIF is made at 90° to the excitation beam. A three-element $f/2.5$ collection optic images a 2-mm segment of the region excited by the laser. A 1-nm FWHM bandpass filter centered at 431 nm is used to reduce flame luminescence while detecting CH fluorescence. The photomultiplier (Hamamatsu H5783) output is sent to a lock-in amplifier for $2f$ detection of LIF at 100 kHz.

The burner is mounted upon vertical and horizontal positioning stages and can also be rotated in the horizontal plane, allowing one to obtain different lines of sight by moving the flame relative to the excitation beam. For most measurements the laser beam is parallel to the slot flame. Second-harmonic CH absorption spectra are acquired by detection of the transmitted beam while the excitation frequency is repetitively swept across the absorption line. The $2f$ signals are calibrated against direct (unmodulated) absorbance measurements along the line of sight of maximum CH absorbance at each flame height.

An etalon fringe equivalent to an absorbance of 5×10^{-4} was observed in the $2f$ spectra and traced to the input and output faces of the doubling crystal. The detection sensitivity is increased by formation of excitation and reference beams prior to the flame by

use of a 50/50 beam splitter, and common mode noise and etalons are removed by subtraction in a dual-channel lock-in amplifier.

Figure 2 shows spectra from direct absorption, $2f$ absorption detection, and $2f$ LIF detection at 2 mm above the burner surface in an ethylene–air flame. Fuel- and air-flow rates are 9.7 and $19.4\text{ cm}^{-3}\text{ s}^{-1}$, respectively, at an atmospheric pressure of 590 Torr and ambient temperature. The peak CH absorbance at this height, as measured by direct absorption, is 7.5×10^{-4} , with a peak-to-peak signal-to-noise ratio (S/N) of 2:1. Assuming a uniform 2000 K flame temperature along the 4-cm-long flame front, and using reported CH electronic transition moments and rotational transition probabilities,¹² we estimate a peak CH mole fraction of 3 parts in 10^6 .

The $2f$ LIF spectrum shown in Fig. 2(c) is taken with the same detection bandwidth and averaging time as the $2f$ absorption spectrum in Fig. 2(b). The WMS and LIF S/N ratios are excellent, and the $2f$ LIF detection scheme is effective in removing interference from flame luminescence. There is a sufficient fluorescence signal for performance of higher-resolution imaging with improved imaging optics and a linear-array detector. As Fig. 2 shows, the use of modulated detection methods provides significant noise reduction relative to unmodulated detection methods.

Figure 3 shows CH concentration profiles, constructed from $2f$ absorption spectra, at flame heights of 2 and 4 mm above the burner surface for ethylene–air and methane–air diffusion flames with equivalent fuel–air mass ratios. A 0-mm lateral position corresponds to the center of the burner, and 4 mm is the position of the fuel–air interface at the burner surface. The peak absorbance decreases and shifts further away from the burner center as the height in the flame increases. The peak CH mole fraction in

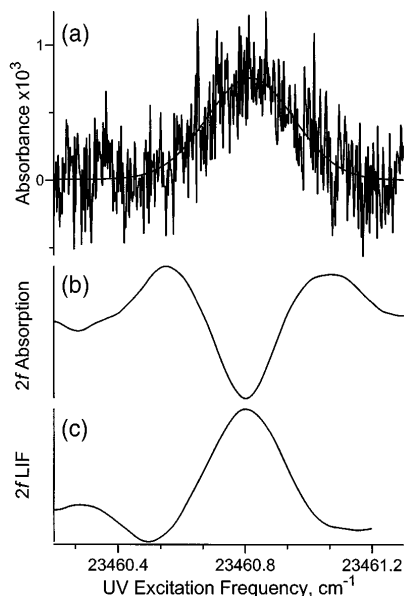


Fig. 2. Monitoring the $R_2(8)$ transition of the CH(0, 0) band of $A^2\Delta \leftarrow X^2\Pi$ transition by (a) direct absorption, (b) $2f$ absorption, and (c) $2f$ LIF detection in an ethylene–air diffusion flame.

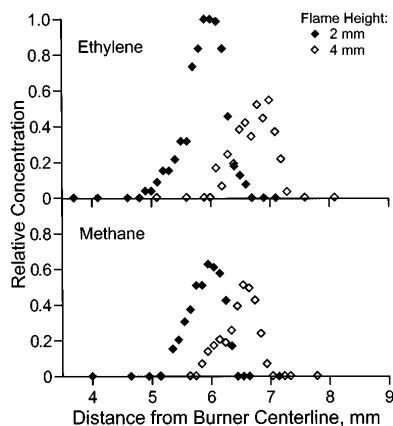


Fig. 3. CH concentration distribution profiles for an ethylene-air diffusion flame and a methane-air diffusion flame at 2 and 4 mm above the burner surface.

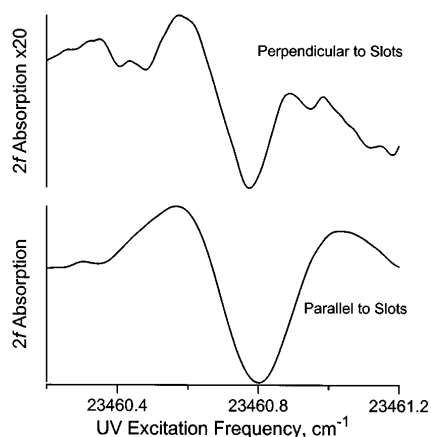


Fig. 4. $2f$ absorption spectra of CH acquired perpendicular and parallel to the flame front.

the methane-air flame at 2 mm is $2/3$ that in the ethylene-air flame.

These peak CH mode fractions are comparable with the 0.08 – 2 -parts-in- 10^6 range estimated by Norton and Smyth⁶ from LIF measurements of a methane-air diffusion flame by use of similar burner and flow rates but at a 9-mm height. They observed similar trends in CH concentration profiles with a change in the flame height. These mole fractions are significantly less than the values of 100 parts in 10^6 or larger reported by others.¹⁰ The accuracy of these concentration determinations can be improved in the future by incorporation of optical thermometry to measure local flame temperatures simultaneously with $2f$ WMS and LIF.

We can reduce the effective path length of CH absorption in the flame to ~ 1.5 mm by turning the flame 90° , thereby simulating a line of sight across a radially symmetric flame. In Fig. 4 we compare the $2f$ absorption signal acquired for this orientation with one taken at the same height but parallel to the diffusion flame front. The perpendicular spectrum is magnified by a factor of 20 and is an average of 1500 sweeps, and the parallel spectrum is an average of 200 sweeps. The upper spectrum shows a peak-to-

peak S/N ratio of $\sim 3:1$ with an absorbance amplitude of 5×10^{-5} . The measurement bandwidth is 3 Hz. Absorbance detection limits of 10^{-6} at a 1-Hz bandwidth are routinely achievable with WMS when care is taken to eliminate source and detector noise and optical etalons from the system.²⁻⁴ In the present apparatus, S/N ratios are limited by etalon fringes and not by source or detector noise. Improvements to the optical components (such as antireflection coatings and nonparallel optical faces) should reduce etalon interference and allow detection limits that approach 10^{-6} without background subtraction.

In conclusion, the feasibility of detecting combustion radicals with simultaneous phase-sensitive, spatially resolved LIF and line-of-sight WMS absorption measurements has been demonstrated in atmospheric-pressure diffusion flames. The WMS measurements afford a quantitative measure of the integrated absorbance along a line of sight with much greater sensitivity than direct absorption measurements. The current lack of single-frequency high-power diode lasers at appropriate wavelengths limits extending this technique to other important combustion species such as OH, NO, and SO_2 . However, by use of power amplifiers and tripling or quadrupling of the outputs, the necessary UV to vacuum ultraviolet wavelengths can be achieved.¹³ In addition, this diode-laser-based approach is suitable for demanding applications such as microgravity drop-tower experiments, in which compact, rugged, energy-efficient instrumentation is required.

This work was supported by the NASA Lewis Research Center under contract NAS3-98044. K. A. Peterson's e-mail address is peterston@swsciences.com.

References

1. N. L. Garland and D. R. Crosley, in *21st Symposium (International) on Combustion* (Combustion Institute, Pittsburgh, Pa., 1986), p. 1693.
2. D. S. Bomse, A. C. Stanton, and J. A. Silver, *Appl. Opt.* **31**, 718 (1992).
3. J. A. Silver, D. J. Kane, and P. J. Greenberg, *Appl. Opt.* **34**, 2787 (1995).
4. D. B. Oh, A. C. Stanton, and J. A. Silver, *J. Phys. Chem.* **97**, 2246 (1993).
5. G. J. Dixon, C. E. Tanner, and C. E. Weiman, *Opt. Lett.* **14**, 731 (1989).
6. T. S. Norton and K. C. Smyth, *Combust. Sci. Technol.* **76**, 1 (1991).
7. C. E. Moore and H. P. Broida, *J. Res. Natl. Bur. Stand. Sect. A* **63**, 19 (1959).
8. K. J. Rensberger, M. J. Dreyer, and R. A. Copeland, *Appl. Opt.* **27**, 3679 (1988).
9. N. L. Garland and D. R. Crosley, *J. Quant. Spectrosc. Radiat. Transfer* **33**, 591 (1984).
10. M. G. Allen, R. D. Howe, and R. K. Hanson, *Opt. Lett.* **11**, 126 (1986).
11. G. A. Raiche and J. B. Jeffries, *Appl. Opt.* **32**, 4629 (1993).
12. J. Luque and D. R. Crosley, *J. Chem. Phys.* **104**, 2146 (1996).
13. J. P. Koplow, D. A. V. Kliner, and L. Goldberg, *Appl. Opt.* **37**, 3954 (1998).